

Effect of Temperature on the Stability of the Precursor Cluster of the Thermolysin Crystal

Yu. V. Kordonskaya^{a,*}, V. I. Timofeev^b, M. A. Marchenkova^{b,c}, Yu. V. Pisarevsky^b, S. Yu. Silvestrova^d,
Yu. A. Dyakova^a, and M. V. Kovalchuk^{a,b}

^a National Research Centre “Kurchatov Institute,” Moscow, 123182 Russia

^b Shubnikov Institute of Crystallography, Kurchatov Complex of Crystallography and Photonics,
National Research Centre “Kurchatov Institute,” Moscow, 119333 Russia

^c The Smart Materials Research Institute, Southern Federal University, Rostov-on-Don, 344090 Russia

^d Loginov Moscow Clinical Scientific Center, Moscow Health Department, Moscow, 111123 Russia

*e-mail: yukord@mail.ru

Received March 25, 2024; revised March 25, 2024; accepted March 30, 2024

Abstract—The stability of the precursor cluster (hexamer) of the thermolysin crystal over a wide temperature range (10–90°C) has been estimated by the molecular dynamics method. The simulation results showed that, with an increase in temperature, the stability of the hexamer generally decreases; however, the hexamer does not dissociate at any of the investigated temperatures. At a temperature of 60°C, an increase in the hexamer stability has been observed. This temperature is close to the temperature of maximum enzymatic activity of thermolysin (70°C). It is suggested, based on the analysis of the results, that the crystallization of thermolysin can be carried out at 60°C.

DOI: 10.1134/S1063774524600480

INTRODUCTION

The functioning of proteins depends to a great extent on their spatial structure, which is most often interpreted by X-ray diffraction analysis. To use this method, a crystal of the protein under study should be grown first. However, the search for the optimum protein crystallization conditions remains a difficult and time-consuming stage, which is still carried out empirically by searching through a large number of conditions. Nevertheless, it was established [1] that the protein crystallization is preceded by the formation of precursor clusters, specifically, 3D fragments of the crystal structure. It was shown that the crystallization conditions (temperature and concentrations of protein and precipitant) determine the formation of clusters and their concentration. Study of the interaction of proteins in precursor clusters can be useful for examining the functioning of proteins, e.g., enzymes. As is known, the protein functioning is based on conformational ensembles [2], the properties of which largely depend on temperature.

It was found [3] that the precursor clusters (dimers) of the crystal of proteinase K, which has the optimum activity at a temperature of 60°C, behave anomalously, and their stability changes abruptly and nonmonotonically as the temperature rises above 60°C. In addition, it was suggested that proteinase K may crystallize at temperatures of ~50°C, which are relatively high for

proteins. In [2], a diffraction set was collected for the proteinase K crystals in the temperature range from 40 to 90°C.

In this work, we used the molecular dynamics (MD) method to investigate the stability of the precursor cluster of the crystal of another thermophilic proteinase, thermolysin, at temperatures from 10 to 90°C, including the temperature of maximum enzyme activity (70°C).

Recent small-angle X-ray scattering studies have confirmed that the precursor clusters forming during thermolysin crystallization are hexamers [4]. In addition, the MD method was used to establish the most stable hexamer type, which is the precursor cluster [5].

Thermolysin is a metalloproteinase produced by the *Bacillus thermoproteolyticus* bacterium. This protein catalyzes the hydrolysis of peptide bonds in proteins and is widely used for peptide mapping and production of peptide fragments for structural and functional investigations. Thermolysin is known for its stability and activity at high temperatures [6]. The catalytic activity of thermolysin is maximum in the pH range of 7.0–9.0 at a temperature of 70°C [7]. The spatial structure contains two domains with an active center between. The thermolysin active site (PDB ID: 3DNZ) includes residues GLU-142, HIS-143, HIS-146, and GLU-166, which coordinate the zinc ion [8].

MATERIALS AND METHODS

Hexamer models were prepared by the technique reported in [3]. Using the crystal structure of hexagonal thermolysin crystals (PDB ID: 3DNZ, sp. gr. $P6_122$), a molecular model of potential growth units of these crystals was created. In the PyMOL molecular graphic system (version 1.8 [9]), using the symmetry operators of the sp. gr. $P6_122$, a thermolysin crystal structure fragment was reconstructed, and the hexamer was isolated from it. The precipitant ions associated with the thermolysin crystal are retained in the hexamer structure (four calcium ions and one zinc ion per protein molecule), while water molecules were removed from the structure file.

To determine the protonation states of the amino acid residues at pH 6.0 (according to the pH value of the crystallization buffer for the crystal with PDB ID: 3DNZ), the PROPKA server (version 3.4.1 [10]) was used. All calculations were carried out in the GROMACS package, version 2021 [11]. In the MD simulation, the Amber ff99SB-ILDN force field [12] was used, in which the torsion potentials for some atomic groups were improved.

Each hexamer was placed at the center of a cubic simulation box with periodic boundary conditions. The minimum distance from the box edge to the protein atom was 1 nm. The boxes were filled with the TIP4P-Ew 4-site water model developed for the use of the Ewald summation methods [13]. The concentration of the ammonium sulfate precipitant in the solution was 0.75 M, as under the crystallization conditions. The 3D structure of the NH_4^+ ion was obtained from PDBChem (code: NH4, [14]) and the 3D structure of the SO_4^{2-} ion using the peptide ligand molecular dynamics (PLMD) module from the MDAnalysis package [15, 16]. Ion topologies were generated in the Antechamber program [17]. To neutralize the total charge of the box, 36 Cl^- ions were added to the solution; this was a necessary condition for applying the PME algorithm in the calculation of long-range electrostatic interactions [18].

Before the productive MD was calculated, the simulated systems were subjected to the energy minimization by the steepest descent method (50 000 steps) until the maximum force per atom became less than 1000 kJ/(M nm). The boxes were then equilibrated for 100 ps using a modified Berendsen (V-rescale) thermostat [19] in the NVT ensemble and equilibrated for 100 ps using a Parrinello–Rahman barostat [20] in the NPT ensemble. The productive MD was calculated in the NPT ensemble with a V-rescale thermostat and a Parrinello–Rahman barostat. The equations of motion were integrated using the standard leapfrog algorithm [21] with a step of 2 fs. The noncovalent interactions were taken into account within the range of 1 nm. The long-range electrostatic interactions were calculated by the particle–mesh Ewald method

(PME, [17]) with the cubic interpolation and a reciprocal space grid step of 0.16 nm. The hexamer bond lengths were fixed using the LINCS algorithm [21].

The length of each calculated trajectory was 100 ns. The molecular dynamics of hexamers was simulated at 10 temperatures from 10 to 90°C with a step of 10°C and at 15°C. Three independent simulations were carried out for each temperature in the range of 10–40°C and at 90°C. For the temperatures from 50 to 80°C, the number of independent simulations was increased to 5.

To perform the structural alignment based on the initial position of thermolysin atoms, the *gmx trjconv* command was used. The root-mean-square fluctuation (RMSF) values were calculated only for C_α atoms using the *gmx rmsf* command. The RMSF values were first averaged (calculating the error from the unbiased variance estimate) for each temperature over the independent simulations (three or five, depending on temperature); after that, the RMSF values and errors (standard deviations) were further averaged over all C_α atoms.

RESULTS AND DISCUSSION

The RMSF values for C_α atoms characterize the flexibility of a polypeptide chain, since they show how much each of these atoms deviates from its average (during the simulation time) site. Large RMSF values and their wide spread indicate instability of the hexamer. Using the simulation data, the RMSF values of C_α atoms were plotted for thermolysin hexamers at all investigated temperatures from 10 to 90°C.

In Fig. 1, the colored curves are plots of the RMSF values of C_α atoms for all simulations on the same scale, and the black curves show the RMSF values averaged over all independent simulations (three for 10–40°C and 90°C or five for 50–80°C) for each specific temperature. It follows from Fig. 1 that, on average, the monomers A and F are most unstable, while the monomers C and D, on the contrary, are the most stable ones. This is explained by the fact that, as can be seen in Fig. 2, the monomers A and F have the smallest contact area with other monomers, while the monomers C and D, on the contrary, are located “deep” in the hexamer.

The black markers in Fig. 1 show the averaged (over simulations) RMSF values for the C_α atoms included in the thermolysin active center. According to Fig. 1, the atoms of the active center are most stable relative to the atoms nearest to them, since the RMSF of the active center takes the smallest values in its vicinity. This suggests that thermolysin can perform its catalytic function even as a part of a precursor cluster at both low and relatively high temperatures (at least up to 90°C).

The results of additional averaging of the RMSF and errors (standard deviations) over all C_α atoms are

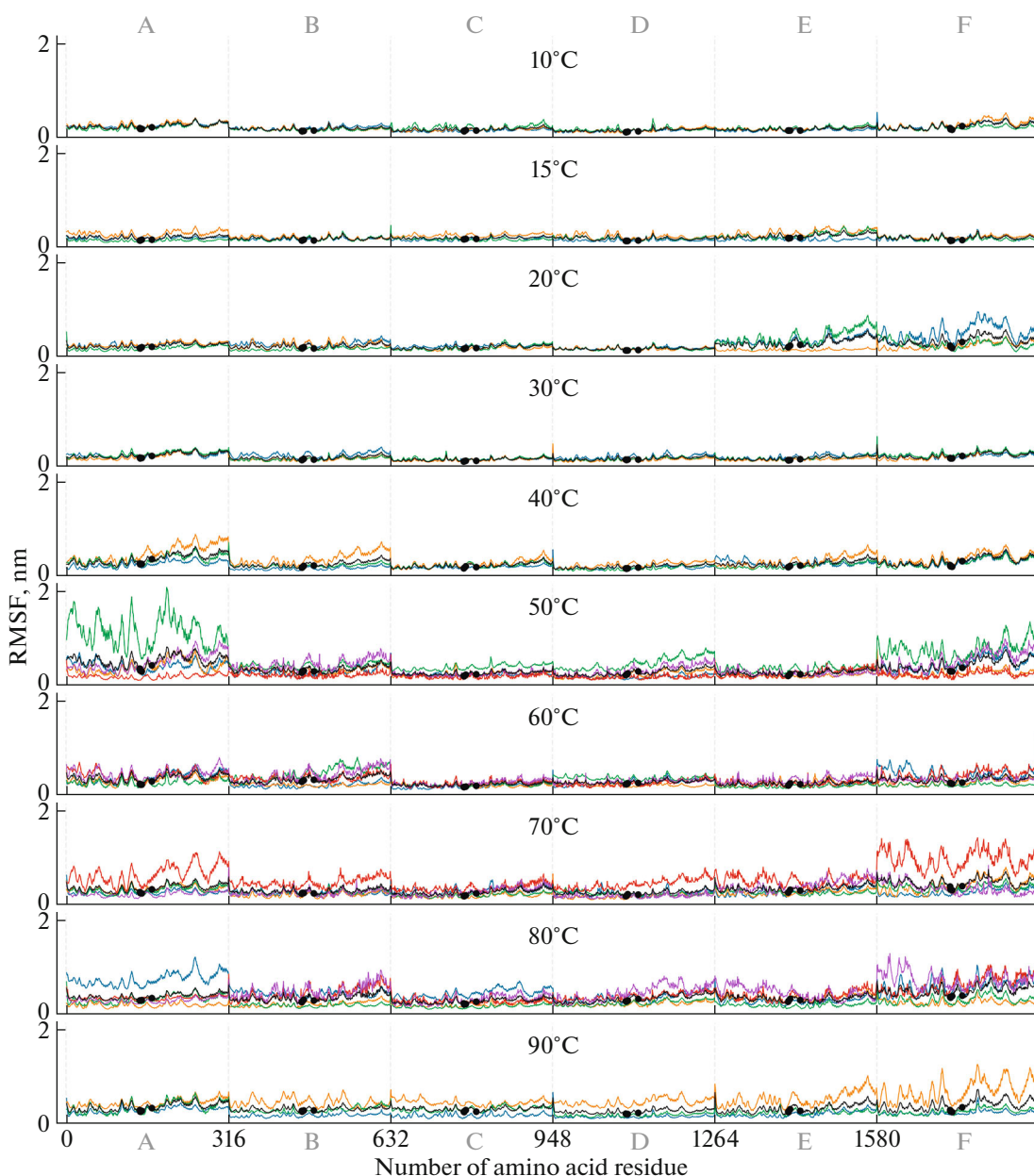


Fig. 1. RMSF values of the precursor cluster (hexamer) of the thermolysin crystal in a crystallization solution at temperatures of 10–90°C. Each colored curve corresponds to one simulation and the black curve corresponds to the RMSF values averaged over all (three or five) independent simulations at a specific temperature.

presented in Fig. 3. It can be seen in Figs. 1 and 3 that the hexamer stability on average decreases with increasing temperature. However, even at a significant mobility of a precursor cluster at high temperatures, analysis of all simulated trajectories showed that the hexamer always remains intact: during the dynamics, any monomer remains associated with the rest hexamer. According to Fig. 1, the greatest transformations in the hexamer structure are observed in one of the simulations at 50°C (green curve in Fig. 1). The next most unstable hexamer was simulated at 70°C (red curve in Fig. 1). The latest frames of the trajectories of

these hexamers (structures after the 100-ns dynamics) are presented in Fig. 4, which shows that not a single molecule managed to separate from the hexamer for 100 ns. Probably, at 50°C, the monomer A, which has the highest RMSF values in Fig. 1, will lose the remaining intermolecular bonds in the nearest future. However, this is the only case out of the 38 simulations in which there is a tendency for at least one monomer to break off. Figure 4 shows that, already in the second most unstable hexamer (at 70°C), all monomers have a sufficiently large area of intermolecular contacts.

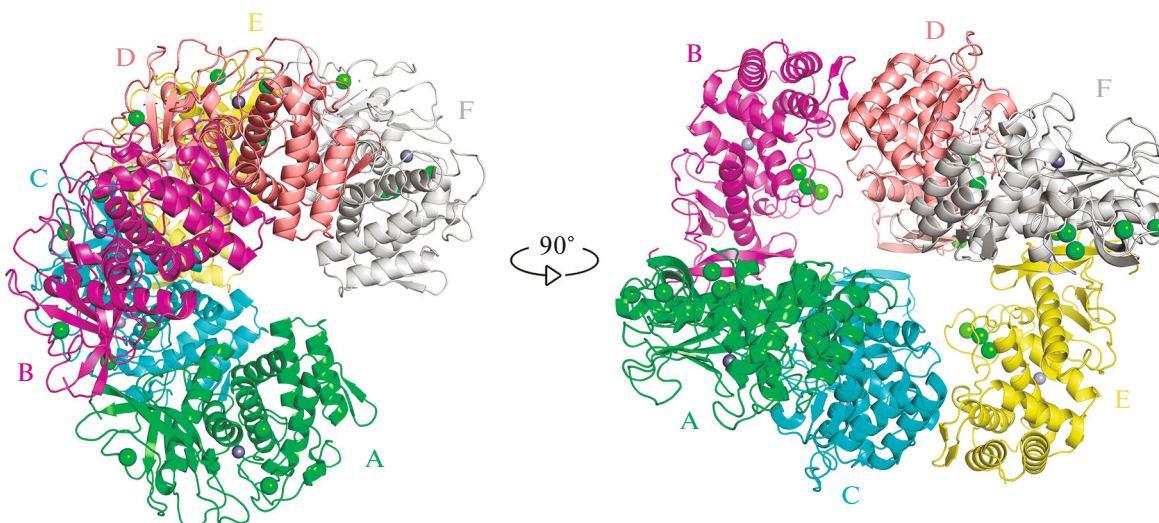


Fig. 2. Precursor cluster (hexamer) of the thermolysin crystal in two projections. Letters A–F indicate the monomers forming the hexamer. Green spheres show calcium ions and gray spheres show zinc ions.

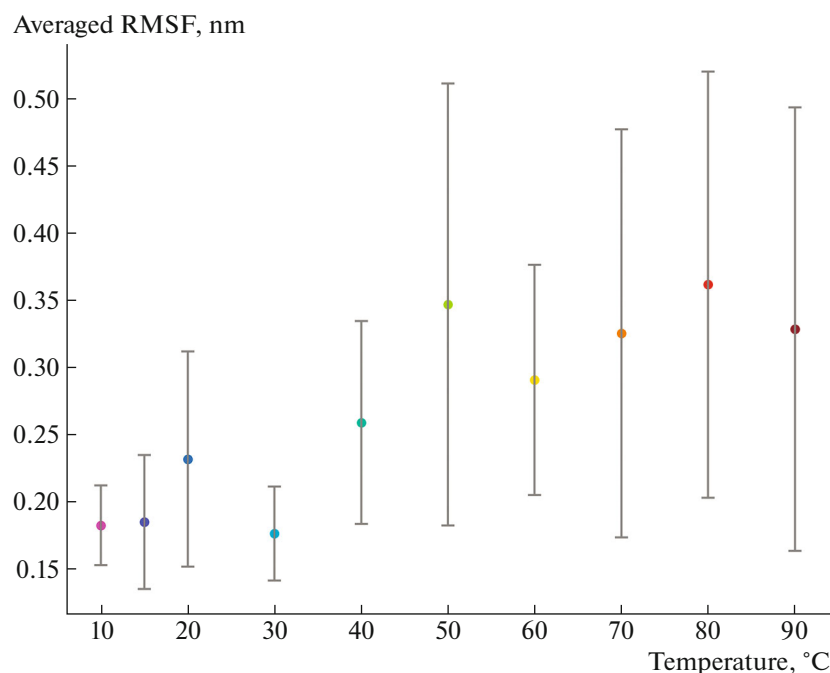


Fig. 3. RMSF values averaged over all C_{α} atoms of the precursor cluster of the thermolysin crystal in a crystallization solution at different temperatures (from 10 to 90°C). The indicated errors form one standard deviation when averaging the RMSF over the independent simulations.

In addition, in a real crystallization solution, a small part of the hexamers also most likely disintegrates.

The integrity of the thermolysin crystal precursor cluster in the range of 10–90°C suggests that its crystallization can be carried out at high temperatures (up to 90°C).

Interestingly, at a temperature of 60°C, which is close to the temperature of the peak thermolysin activ-

ity (70°C [7]), the spread of the RMSF values around the mean is minimum in the temperature range from 50 to 90°C (Fig. 3). The RMSF range at 60°C is almost 2 times narrower than those at temperatures of 50, 70, 80, and 90°C. The narrow RMSF spread at 60°C indicates that the degree of the protein stability at this temperature is maintained somewhat better (over five independent simulations) than at other tem-

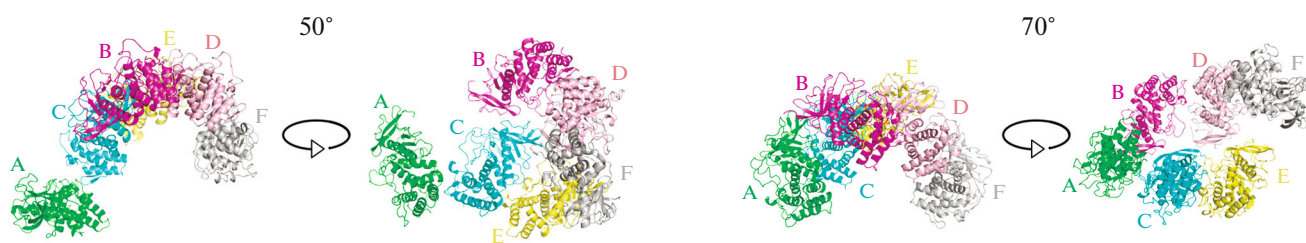


Fig. 4. Least stable hexamers at the end of the simulation (100 ns) in two projections at 50°C (on the left) and 70°C (on the right). Thermolysin molecules do not detach from the hexamer even during the MD of the most unstable structures.

peratures in the range of 50–90°C. This may indicate the increased reproducibility of the simulation at a temperature close to that of the maximum enzymatic activity of thermolysin, i.e., better predictability of the behavior of protein at this temperature. In addition, according to [3], for another protease (proteinase K), not only the absolute RMSF value remained relatively low but also the RMSF range was quite narrow precisely at the temperature corresponding to the maximum enzymatic activity of proteinase K. This indicates a possible general property of proteases: the relative stability of the precursor clusters of their crystals at temperatures close to their peak activity temperature.

CONCLUSIONS

The effect of temperature (from 10 to 90°C) on the stability of a precursor cluster of the thermolysin crystal was studied by the MD method. It was found that the stability of the hexamer decreases on average with increasing temperature, but its integrity is maintained. It was noted that, at a temperature of 60°C, which is close to the temperature of thermolysin peak activity (70°C), the RMSF spread around the average is minimum in the range from 50 to 90°C. This fact suggests that crystallization of thermolysin can be carried out at 60°C, since the precursor clusters are quite stable at this temperature.

ACKNOWLEDGMENTS

This work has been carried out using computing resources of the federal collective usage center Complex for Simulation and Data Processing for Mega-science Facilities at NRC “Kurchatov Institute,” <http://ckp.nrcki.ru/>.

FUNDING

This study was carried out within the framework of the State assignment of the National Research Center “Kurchatov Institute” and with the support of the Ministry of Science and Higher Education (grant no. 075-15-2021-1363 (continued)).

CONFLICT OF INTEREST

The authors of this work declare that they have no conflicts of interest.

REFERENCES

1. M. A. Marchenkova, A. S. Boikova, K. B. Ilina, et al., *Acta Nat.* **15** (1), 58 (2023). <https://doi.org/10.32607/ACTANATURAE.11815>
2. S. Du, S. A. Wankowicz, F. Yabukarski, et al., *bioRxiv* (2023). <https://doi.org/10.1101/2023.05.05.539620>
3. Y. V. Kordonskaya, V. I. Timofeev, Y. A. Dyakova, et al., *Crystals* **12** (11), 1645 (2022). <https://doi.org/10.3390/CRYST12111645>
4. M. V. Kovalchuk, A. S. Boikova, Y. A. Dyakova, et al., *J. Biomol. Struct. Dyn.* **37** (12), 3058 (2019). <https://doi.org/10.1080/07391102.2018.1507839>
5. Y. V. Kordonskaya, V. I. Timofeev, Y. A. Dyakova, et al., *Mend. Commun.* **33** (2), 225 (2023). <https://doi.org/10.1016/J.MENCOM.2023.02.024>
6. B. van den Burg and V. Eijsink, *Handb. Proteolytic Enzymes* **1**, 540 (2013). <https://doi.org/10.1016/B978-0-12-382219-2.00111-3>
7. M. P. Y. Lam, E. Lau, X. Liu, et al., *Comprehensive Sampling and Sample Preparation: Analytical Techniques for Scientists* (2012), p. 307. <https://doi.org/10.1016/B978-0-12-381373-2.00085-5>
8. O. A. Adekoya and I. Sylte, *Chem. Biol. Drug. Des.* **73** (1), 7 (2009). <https://doi.org/10.1111/J.1747-0285.2008.00757.X>
9. W. L. DeLano, *The PyMOL Molecular Graphics System, Version 1.8* (Schrödinger, LLC, New York, NY, USA, 2015).
10. E. Jurrus, D. Engel, K. Star, et al., *Protein Sci.* **27** (1), 112 (2018). <https://doi.org/10.1002/PRO.3280>
11. D. Van Der Spoel, E. Lindahl, B. Hess, et al., *J. Comput. Chem.* **26** (16), 1701 (2005). <https://doi.org/10.1002/jcc.20291>
12. K. Lindorff-Larsen, S. Piana, K. Palmo, et al., *Proteins: Struct., Funct., Bioinf.* **78** (8), 1950 (2010). <https://doi.org/10.1002/prot.22711>
13. H. W. Horn, W. C. Swope, J. W. Pitera, et al., *J. Chem. Phys.* **120** (20), 9665 (2004). <https://doi.org/10.1063/1.1683075>

14. D. Dimitropoulos, J. Ionides, and K. Henrick, *Curr. Protoc. Bioinf.* **14.3.1** (2006).
15. N. Michaud-Agrawal, E. J. Denning, T. B. Woolf, and O. Beckstein, *J. Comput. Chem.* **32** (10), 2319 (2011).
<https://doi.org/10.1002/JCC.21787>
16. R. J. Gowers, M. Linke, J. Barnoud, et al., *15th Python in Science Conference, Los Alamos, NM (United States), September 11, 2016*, p. 98.
<https://doi.org/10.25080/Majora629e541a-00e>
17. A. W. Sousa Da Silva and W. F. Vranken, *BMC Res Notes* **5** (1), 1 (2012).
<https://doi.org/10.1186/1756-0500-5-367/FIG-URES/3>
18. U. Essmann, L. Perera, M. L. Berkowitz, et al., *J. Chem. Phys.* **103**, 8577 (1995).
<https://doi.org/10.1063/1.470117>
19. H. J. C. Berendsen, J. P. M. Postma, W. F. Van Gunsteren, et al., *J. Chem. Phys.* **81** (8), 3684 (1984).
<https://doi.org/10.1063/1.448118>
20. M. Parrinello and A. Rahman, *J. Chem. Phys.* **76** (5), 2662 (1982).
<https://doi.org/10.1063/1.443248>
21. W. F. Van Gunsteren and H. J. C. Berendsen, *Mol. Simul.* **1** (3), 173 (1988).
<https://doi.org/10.1080/08927028808080941>
22. B. Hess, H. Bekker, H. J. C. Berendsen, and J. G. E. M. Fraaije, *J. Comput. Chem.* **18**, 1463 (1997).
[https://doi.org/10.1002/\(SICI\)1096-987X\(199709\)18:12<1463::AID-JCC4>3.0.CO;2-H](https://doi.org/10.1002/(SICI)1096-987X(199709)18:12<1463::AID-JCC4>3.0.CO;2-H)

Translated by E. Bondareva

Publisher's Note. Pleiades Publishing remains neutral with regard to jurisdictional claims in published maps and institutional affiliations.

AI tools may have been used in the translation or editing of this article.